Robust Visual Servoing Control with a Humanoid Robot for Performing Chinese Calligraphy

Ma Zhe [1,2], Xiang Zhenzhen [1,2], Su Jianbo [1,2†]

1.*Department of Automation, Shanghai Jiao Tong University , Shanghai 200240, China;*

2.*Key Laboratory of System Control and Information Processing, Ministry of Education, Shanghai 200240, China*

Abstract:

An uncalibrated visual servoing system is described with a humanoid robot for Chinese calligraphy. The system is designed based on Kalman-Bucy filter with the help of object detector by Continuously Adaptive MeanShift (CAMShift) algorithm. Under this control scheme, a humanoid robot could perform satisfactorily in grasping a brush and writing strokes in sequences according to the structure of Chinese characters, despite the inaccuracy in system modeling. The proposed method is shown to be robust and effective in its performance through a task of Chinese calligraphy by the NAO robot.

Keywords: Robust visual servoing; Kalman-Bucy filter; CAMShift algorithm

0 Introduction

Endowing robots with humanoid ability is essential for robots to be accepted in human society more easily [1-4]. Besides various applications, it is expected that the robot could provide special entertainment and assistance for people. Chinese calligraphy is an advanced skill for human beings in Chinese civilization along Chinese history of more than 5000 years. It is an art expressing the emotion and aesthetics of the author. It will be useful and encouraging if robots could write Chinese calligraphy like humans do.

Since the writing brush specially designed for Chinese calligraphy is soft, strokes of different and variable widths can be drawn. In fact, slight changes in the strength, orientation as well as moving speed exerted on the brush can result in quite different effects. Hence, Chinese calligraphy writing is basically movements in three dimensions instead of two. A thick stroke can be written through pressing the brush heavily [5]. Whether a sharp corner or a smooth corner can be formed in a stroke depends on how the author rotates the writing brush. A blurred stroke comes from fast speed [6]. These characteristics bring huge difficulties to Chinese calligraphy and simultaneously make Chinese calligraphy a charming art [7].

There have been many efforts to enable robots the ability of performing Chinese calligraphy. Yao and Shao [6] presented the modeling of Chinese characters achieved through thinning the image, detecting the skeleton and modeling the skeleton with B-splines. This modeling works well on ancient style Chinese character calligraphy and is shown to be effective on a manipulator. However, this method only deals with the trajectories of strokes and ignores the changes in width of strokes and the orientation of the brush. Lam and Yam [8] described a technique to generate stroke trajectories and proved it to be effective on a 5-DOF robotic art system. Herein, the stroke locus is represented by footprints along it. The changes in stroke width are taken into account in the water-droplet-like model of footprint, whereas the brush is limited to move in longitudinal direction. Besides, strokes written in this way are not so smooth due to the discrete footprints. Zhang and Su [9] proposed a sensor management model, which is based on fuzzy decision tree (FDT). The model can integrate necessary prerequisite knowledge of Chinese calligraphy and is verified on an Adept 604S robot manipulator. Nevertheless, the proposed model is implemented on a manipulator with 4DOF instead of a humanoid robot. These efforts have three mutual problems. First, the orientation of the brush is fixed during writing, which will limit the writing performance. Second, all these researches are implemented on manipulators without human-robot interaction. Third, the workspace is restricted by the fixed base of the robot.

†Corresponding author.

E-mail: jbsu@sjtu.edu.cn. Tel.: +86 136 6179 3223.

This work was supported by National Natural Science Foundation of China under the grant 61221003.

Compared with enabling manipulators the ability of performing Chinese calligraphy, allowing humanoid robots to perform it has more advantages. Humanoid robots can be accepted by humans in quotidian lives more easily due to their appearance. Therefore, humanoid robots with the skill of performing Chinese calligraphy can teach children writing and amuse elderly people. Furthermore, the workspace of humanoid robots can be expanded larger than that of manipulators because they can walk around, and consequently the space of writing is enlarged. In addition, humanoid robots can keep learning different kinds of strokes through interaction with humans.

A complete writing task on a humanoid robot includes grasping [10-13] and writing with a brush. There are some challenges in this task. Compared with models of a manipulator, less accuracy will be obtained by those of a humanoid robot, involving vision model and the relationship between visual space and workspace. Therefore, uncalibrated visual servoing control [14][15] is the key technique to ameliorate grasping performance. Besides, different from manipulators which are fixed firmly on tables, a humanoid robot stands on two feet like human beings. Hence the body will shake slightly when its hand is moving, which will bring noises to images and disturbances to the motion system. Such noises and disturbances will deteriorate visual servoing control. In addition, the brush handed by the person may move in an irregular track, which is challenging for object detectors to handle.

In this paper, a complete task of Chinese calligraphy with a humanoid robot is explored. The robot is supposed to grasp a brush handed by a person and then write a Chinese character. A robust uncalibrated visual servoing system based on Kalman-Bucy filter [16] with the help of an objector detector by Continuously Adaptive MeanShift (CAMShift) algorithm [17] is described to implement this task. Finally experiment is carried on with the NAO robot [18] using the described approach and the results verifies the robustness to noises in images, disturbances on motion and irregular target trajectory.

The rest of this paper is organized as follows. In Section II, a robust visual servoing system is described, including the whole structure, object detection technique based on CAMShift algorithm and an uncalibrated visual servoing controller based on Kalman-Bucy filter. Experiments on a humanoid robot, NAO, using the proposed method and the partitioned Broyden's algorithm are presented in Section III respectively to verify the performance of the proposed method. Finally, conclusions and future work are given in Section IV.

1 Robust visual servoing system

1.1 System structure

The visual servoing system proposed in this paper is expressed in the form of diagram in Fig. 1. As indicated in the diagram, the state estimator based on Kalman-Bucy filter estimates image Jacobian matrix using control quantity exerted on the robot and image features of robot end-effector. Herein, the image features are captured by CAMShift algorithm, and the image Jacobian matrix is used to calculate the control quantity for the next control period. Future image features of robot end-effector act as set values of the control circle and can be predicted with the present and past values.

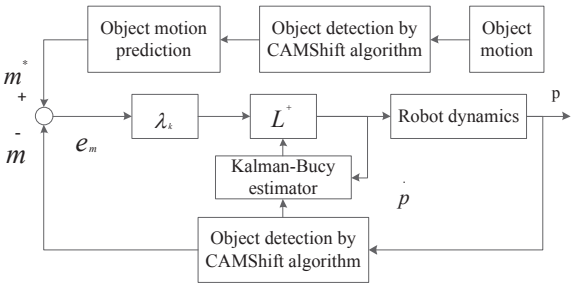

Fig. 1 Robust visual servoing system .

1.2 Object detection

CAMShift algorithm was derived from the earlier Meanshift algorithm [19] and aims at detecting objects in continuous video. According to CAMShift algorithm, the center of mass of the target object is calculated through MeanShift algorithm using color feature. The range of the target object in current image is figured out by adjusting the size of the searching window, and this range information is used to set original searching window in the next image. By repeating this process, the target object is tracked continuously. The block diagram of CAMShift algorithm is as Fig. 2 shows. The specific process of CAMShift algorithm is as follows [17]:

(1) Transform the captured RGB image into an HSV image.
(2) Set original tracking area of the target object, and set searching window.
(3) According to MeanShift algorithm, pick up H(hue) channel from HSV images to form a new grey image. And histogram of a selected searching area in this grey image, called hue histogram of the corresponding area in the original image, is built. Taking this histogram as searching table, H channel of the

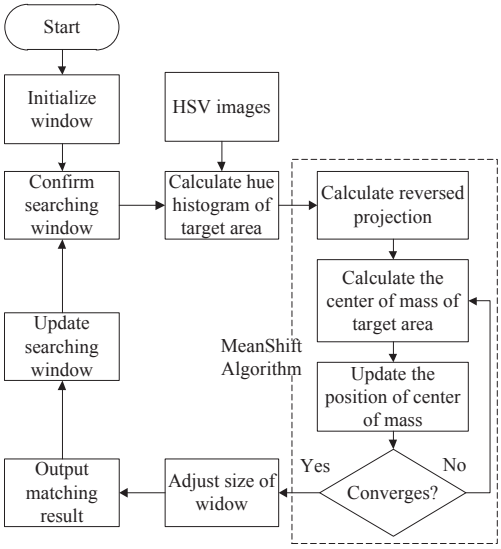

Fig. 2 Block diagram of CAMShift algorithm [17].

original image is mapped into a new grey image (back-projection image). Then the center of mass of searching area in this new image is calculated. Calculate two-order moment $M_{02} = \Sigma_u \Sigma_v v^2 \cdot I(u,v)$, $M_{20} = \Sigma_u \Sigma_v u^2 \cdot I(u,v)$, where u and v are the coordinates of the pixel in the image. Based on zero-order moment, one-order moment, two-order moment, deflecting angle of the target object can be calculated:

$$\theta = arctan(\frac{2 \times (\frac{M_{11}}{M_{00}} - u_c v_c)}{(\frac{M_{20}}{M_{00}} - u_c^2) - (\frac{M_{02}}{M_{00}} - v_c^2)})/2, \quad (1)$$

where u_c and v_c are the coordinates of the pixel in the image.

(4) Adjust the size of searching window according to the calculation below:

$$a = \frac{M_{20}}{M_{00}} - u_c^2, \quad (2)$$

$$b = 2(\frac{M_{11}}{M_{00}} - u_c v_c), \quad (3)$$

$$c = \frac{M_{02}}{M_{00}} - v_c^2, \quad (4)$$

$$r = \sqrt{\frac{(a+c) + \sqrt{b^2 + (a-c)^2}}{2}}, \quad (5)$$

$$s = \sqrt{\frac{(a+c) - \sqrt{b^2 + (a-c)^2}}{2}}, \quad (6)$$

where r and s represent length and width of new tracking window, respectively.

(5) Determine whether coordinate of center of mass converges or not according to MeanShift algorithm. If it converges, go to step (6), otherwise calculate new center of mass and set it as the center of searching window, then go to step (3).

(6) Output detection result, and update tracking window and searching window, then go to step (1).

The center of mass of the searching window represents the position of the object, which refers to the right hand of the robot or the brush in our task. The coordinates of this point will construct visual features and be used to calculate control quantity in the visual servoing control.

1.3 Uncalibrated visual servoing control based on Kalman-Bucy filter

To estimate image Jacobian matrix with Kalman-Bucy filter, the model of visual servoing system should be transformed into the form of state function of linear system. Herein, the system state is formed with the members of image Jacobian matrix and the system output is the changes in visual features. Since Kalman-Bucy filter is tolerant of noises on system state and system output in a linear system, the visual servoing control method based on Kalman-Bucy filter is tolerant of the disturbances on the visual servoing system and noises on the images accordingly.

The model of the visual servoing system based on image Jacobian is defined as follows:

$$\dot{m} = L(p) \cdot \dot{p}, \quad (7)$$

where

$$L(p) = \frac{\partial m}{\partial p} = \begin{pmatrix} \frac{\partial m_1(p)}{\partial p_1} & \cdots & \frac{\partial m_1(p)}{\partial p_n} \\ \vdots & \ddots & \vdots \\ \frac{\partial m_l(p)}{\partial p_1} & \cdots & \frac{\partial m_l(p)}{\partial p_n} \end{pmatrix}_{l \times n}. \quad (8)$$

Herein, $m \in R^l$ presents the visual feature of robot end-effector in images, $p \in R^n$ represents the coordinate of robot end-effector in task space, $L(p) \in R^{l \times n}$ represents the image Jacobian matrix, which is unknown in uncalibrated visual servoing and needs to be estimated through Kalman-Bucy filter. Transforming equation (7) into discrete form, we get

$$m(k+1) \approx m(k) + L(p(k)) \cdot \triangle p(k). \quad (9)$$

A vector, x, is constructed with elements of the image Jacobian matrix as follows:

$$x = ((\frac{\partial m_1}{\partial p})^T (\frac{\partial m_2}{\partial p})^T \ldots (\frac{\partial m_l}{\partial p})^T)^T, \quad (10)$$

where $\frac{\partial m_i}{\partial p} = (\frac{\partial m_i}{\partial p_1}\frac{\partial m_i}{\partial p_2}\dots\frac{\partial m_i}{\partial p_n})^T (i = 1, \dots, l)$ is the transpose of a row of the image Jacobian matrix $L(p)$. Besides, another vector, y, is defined as the change of image feature caused by movement of robot end-effector:

$$y(x) = m(k+1) - m(k), \tag{11}$$

Treating x as the state vector, y as the output vector, and substituting (10),(11) into (9), we get the state function of the system:

$$\begin{cases} x(k+1) = x(k) + \eta(k) \\ y(k) = H(k)x(k) + w(k), \end{cases} \tag{12}$$

where $\eta(k)$, $w(k)$ present state noise and observing noise of the above linear system respectively, which are assumed to be independent white Gauss noises satisfying:

$$\begin{cases} E(\eta(k)) = 0 \\ cov\{\eta(k), \eta(j)\} = R_\eta \delta_{kj} \\ E(w(k)) = 0 \\ cov\{w(k), w(j)\} = R_w \delta_{kj} \\ cov\{\eta(k), w(j)\} = R_{\eta w} = 0, \end{cases} \tag{13}$$

and

$$H(k) = \begin{pmatrix} \Delta p(k)^T \dots & 0 \\ \vdots & \ddots \quad \vdots \\ 0 & \dots \Delta p(k)^T \end{pmatrix}_{l \times ln}. \tag{14}$$

Then, the image Jacobian matrix is estimated as the state of system through Kalman filter [15]:

$$G(k+1) = F(k) + R_\eta, \tag{15}$$

$$K(k+1) = G(k+1)H(k)^T[H(k)G(k+1)H(k)^T + R_w]^{-1}, \tag{16}$$

$$F(k+1) = [I - K(k+1)H(k)]G(k+1), \tag{17}$$

$$\hat{x}(k+1) = \hat{x}(k) + K(k+1)[y(k+1) - H(k)\hat{x}(k)], \tag{18}$$

where $\hat{x}(k)$ is the estimated value of x in time k, $K(k+1)$ is the Kalman gain matrix, $G(k+1)$ is covariance matrix of the predicted error, $F(k+1)$ is the covariance matrix of filter error in the theory of Kalman filter. The initialized value, $\hat{x}(0)$, which is constructed with the members of the initialized image Jacobian matrix, can be calculated by least square algorithm with image feature changes caused by a three-step trial movement [16].

After estimating the image Jacobian matrix, the control quantity to control end-effector of the robot can be calculated next. Herein, we get the control quantity in discrete form:

$$u(k) = \triangle p^g(k) = \hat{L}(k)^+(m^*(k) - m^g(k)), \tag{19}$$

where $m^*(k)$ is the expected image feature of the end-effector of the robot, $m^g(k)$ is the image feature of the target object, $\hat{L}(k)^+$ is the Moore-Penrose inverse matrix of the estimated image Jacobian matrix $\hat{L}(k)$. $m^*(k)$ can be approximated by the estimated image feature of the object in the next period, $\hat{m}^o(k+1)$, which can be calculated through one-order prediction:

$$\hat{m}^o(k+1) = m^o(k) + (m^o - m^o(k-1)) = 2m^o(k) - m^o(k-1). \tag{20}$$

Define $e_m(k) = \hat{m}^o(k+1) - m^g(k)$, and consider the boundary of end-effector's velocity, then control quantity is adjusted into:

$$u(k) = \lambda_k \cdot \hat{L}(k)^+ \cdot e_m(k), \tag{21}$$

where

$$\lambda_k = min(\frac{\|\triangle p_{max}\|}{\|\hat{L}(k)^+ \cdot e_m(k)\|}, 1). \tag{22}$$

Herein, $\triangle p_{max}$ is the upper limit of moving velocity of robot's end-effector, so that the control quantity doesn't exceed robot's moving capacity.

2 Experiments

A visual servoing system is presented for humanoid robots in this paper. To verify this approach, a task of Chinese calligraphy is designed and implemented in this section. This task includes two phases. The robot reaches for and grasps a brush handed to it by a participant in the first phase and writes Chinese characters with the brush in the second phase. The former phase is done using the visual servoing system described in this paper while the latter phase is done with the motion generator through demonstration provided by Aldebaran Robotics.

The experiment platform is designed as shown in Fig. 3. This system mainly consists of a NAO robot, a laptop and two USB cameras which are fixed on the NAO robot's head. In the task, the NAO robot's right arm is controlled to grasp the brush and finally write Chinese character. This arm has 6 DOFs including 2 in shoulder, 2 in elbow, 1 in wrist, and one in hand. Since there is no shared view field between the NAO robot's own eyes which are embedded on its face, we fix two cameras on NAO robot's head to endow the robot with stereo vision.

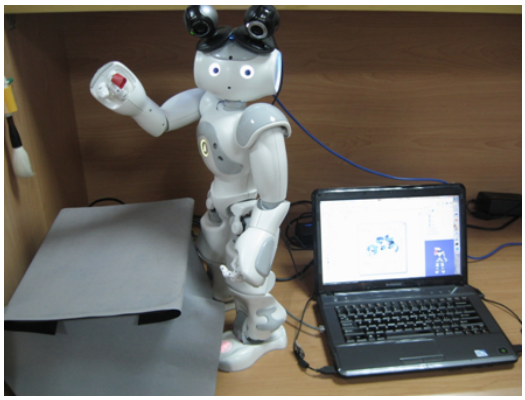

Fig. 3 Experiment platform based on the NAO robot.

The visual servoing task on this platform is done through two parallel processes. One process is on laptop, which captures images, executes image processing and calculates control quantity. The other one is done by the NAO robot, which plans motion and controls robot's right arm. Fig. 4 is a schematic drawing that illustrates the two working parallels. Herein, the computer captures images through two cameras and detects object from these images. Then we get the positions of the right hand of the NAO robot and the brush from the view of the two cameras. These positions are used as image features to estimate Jacobian matrix online in subsequent visual servoing calculation. With Jacobian matrix, control quantity is calculated and sent to the NAO robot through Ethernet. Finally the NAO robot plans its motion and control its right hand to reach for and grasp the brush.

The values of essential parameters in the experiment are given in table 1. Herein, the maximal velocity in the table represents the maximal velocity of the NAO's hand in every coordinate direction. $P(0)$, R_η, and R_w are parameters in visual servoing control method based on Kalman-Bucy filter.

Table 1 Essential Parameters for the experiment.

Parameter	Value
Resolution of images	320×240 $(pixel)$
Maximal velocity	1 cm/s
$F(0)$	10^{-2} I_{12}
R_η	50 I_{12}
R_w	500 I_4
Control period	0.8 s

2.1 Object detection

In the beginning, experiment is carried out to verify the robustness of the object detection technique in the tracking strategy proposed in this paper. In this section, the end-effector of the NAO robot's arm is controlled to move before a complex background consisting of objects of different shapes and colors. The CAMShift algorithm is utilized to detect and localize the moving end-effector in the image captured by one camera of the visual servoing system. The detecting result is shown in Fig. 5, where a red circle marks the detected end-effector and the center of the circle represents the position of the detected end-effector. It can be seen from the figure that the end-effector is detected correctly and the performance of the algorithm is rarely effected by the background. The position of the detected object changes within several pixels. It should be pointed out that there is object with the same color, red, of the end-effector in the background and the end-effector move across the red area in the image. Since hue(H) channel of HSV image is employed in detection, the existence of the red object brings challenge to this task. When the end-effector is moving by the red object, the target area in CAMShift algorithm is extended to contain the object. Nevertheless, new addition in the area only adjusts the size in limited level. When the end-effector moves away, the target area is back to the end-effector.

2.2 Brush grasping

In this experiment, the brush is moving in an irregular track, and the velocity is around 1cm/s. The task is to detect, track and finally grasp the brush with robot's right hand. After completing the task with the visual tracking strategy proposed in this paper, a comparison experiment between our strategy and a classical visual servoing method[15] combined with CAMShift algorithm is carried out to verify the performance of our strategy. To simplify calculation and raise tracking speed, marks in different colors are made on the robot's hand and target to be detected by cameras.

Original positions of NAO's right hand in images are $[172, 168]$(pixel) for left camera and $[192, 174]$(pixel) for right camera. Original positions of target object in images are $[270, 115]$(pixel) for left camera and $[272, 31]$(pixel) for right camera.

Considering that the value of image Jacobian matrix varies as the position and orientation of the robot's end-effector changes, the initialized value of image Jacobian matrix is calculated according to the position and orientation of the NAO robot's hand at the beginning of the experiment. Control NAO's hand to make a three-step trial movement from the beginning position. Making use of the coordination changes of NAO's right hand in images cap-

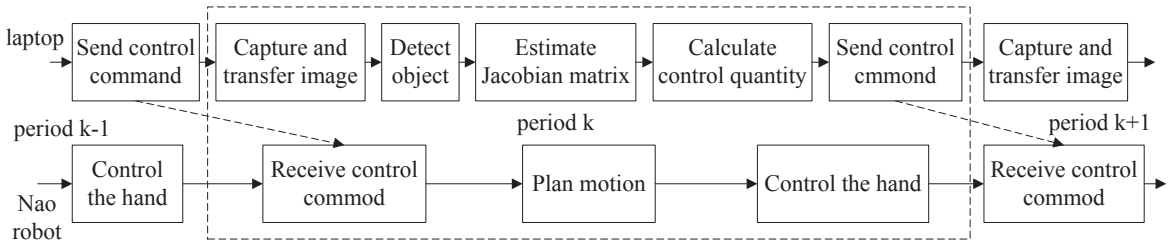

Fig. 4 Flow char of visual servoing control on the NAO robot.

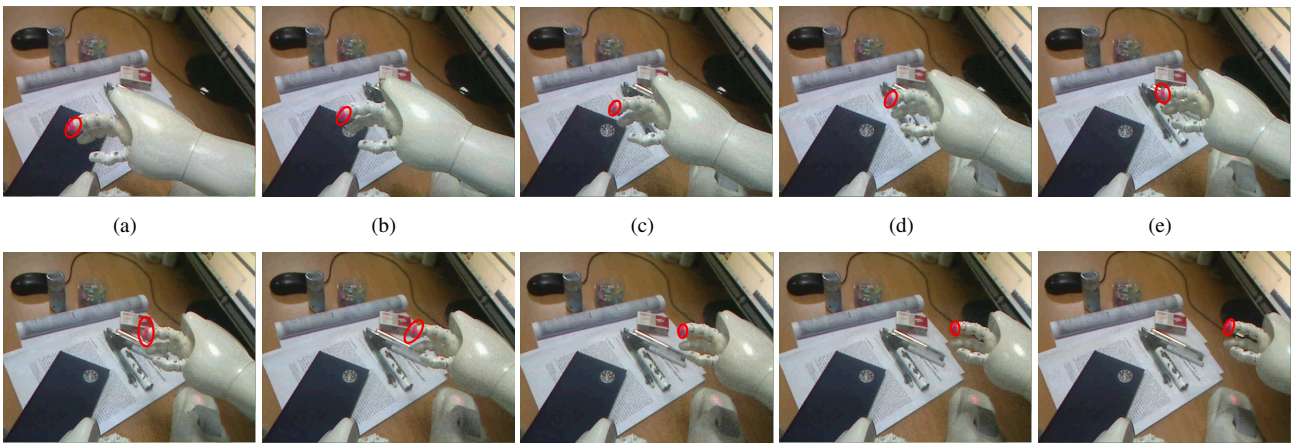

Fig. 5 Moving end-effector detection in complex background.

tured from the two cameras during the trial movement, original value of image Jacobian matrix is calculated. According to the relation $\dot{m} = L\dot{p}$, we get $\Delta m = L\Delta p$, where Δm and Δp represent changes in image feature and Cartesian coordination, respectively. Then the nominal image Jacobian matrix is achieved through $\hat{J}(0) = [\Delta m_1, \Delta m_2, \Delta m_3][\Delta p_1, \Delta p_2, \Delta p_3]^T$. The matrix calculated here is

$$\hat{L}(0) = \begin{pmatrix} 228.4 & -1005.7 & 1079.2 \\ -2646.5 & -364.6 & 452.1 \\ -459.9 & -1470.7 & -882.7 \\ -2304.7 & 570.6 & 498.2 \end{pmatrix}. \quad (23)$$

Fig. 6 describes how NAO's hand tracks the brush. During the task, the binocular vision system captures images of the task space. The NAO's hand and the brush are detected and located in the images through CAMShift algorithm according to the tracking strategy proposed in this paper. Then the task is characterized in the visual space. In the very beginning, the image error between the mark on NAO's hand and the brush is 111 pixels observed from the left camera and 163 pixels from the right camera. The image Jacobian is estimated according to Kalman-Bucy estimator iteratively, based on which control instructions are obtained. NAO's hand tracks the mark on the brush with the control instructions. The control quantities are reducing as the distance between NAO's hand and the brush becomes smaller. Finally, NAO's hand reaches to the brush in 17 steps. Image errors between marks on NAO's hand and the brush in the end of tracking process are within 10 pixels which are caused by the sizes of target object and NAO's hand.

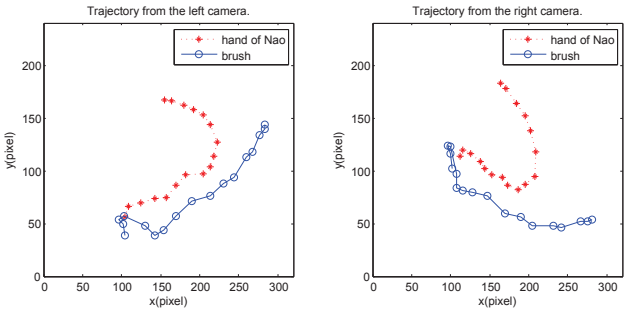

Fig. 6 Brush tracking trajectories in the stereo vision system.

The experimental results verify that the NAO robot can track a moving target accurately with its hand using the proposed visual servoing system. This approach is shown

to be robust to image noises, disturbances caused by slight shake of NAO's body and irregular object motion.

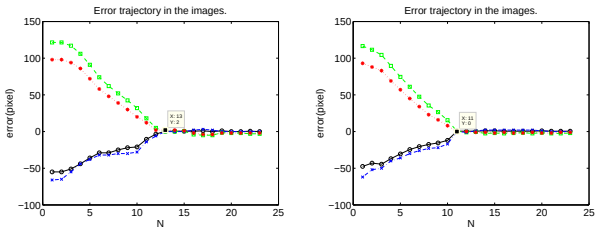

(a) (b)

Fig. 7 Tracking errors observed from two cameras. (a) is obtained using the partitioned Broyden's method; (b) is obtained using the strategy in this paper.

Then our tracking strategy consisting of CAMShift algorithm and Kalman-Bucy filter-based visual servoing control method is compared with the partitioned Broyden's method combined with CAMShift algorithm here. NAO's hand is controlled from the same position in the robot coordinate to track the same point with these two strategies, respectively. The initial position of the hand's end-effector observed from the two cameras are (184, 89) pixel and (99, 56) pixel, respectively. The initial position of the target point observed from the two cameras are (184, 89) pixel and (99, 56) pixel, respectively. The control results are shown in Fig. 7. It can be seen from the figure that the strategy based on the partitioned Broyden's method converges in 13 steps while the strategy proposed in this paper converges in 11 steps. In addition, the tracking error in every direction in the image can reach 4 pixels using the partition's method while error is within 1 pixel utilizing our strategy. The visual tracking strategy presented in this papre is validated to be accurate, fast and robust against noises and disturbances for such interaction task on humanoid robots.

2.3 Writing with a brush

In this task, the NAO robot reaches for and grasps a brush handed to it with its right hand using the visual servoing system proposed in this paper and writes Chinese characters on paper with the brush. The writing phase of the task is realized by motion generator through demonstration using Choregraphe software provided by Aldebaran corporation.

The positions of NAO's hand and the brush from the view of the two cameras in the beginning and the end of the task are shown in Fig. 8, where red circles and green circles indicate NAO robot's right hand and the brush detected by CAMShift algorithm described in this paper, respectively. The writing result is shown in Fig. **??**. These two characters, Jiao and Da, are written according to the requirement of Chinese calligraphy, thereby reflecting certain meanings and emotions. The strokes and structures of these two characters are symmetrical, which is appreciated very much in the aesthetic of Chinese traditional civilization. The character, Jiao, which looks like a smiling face, indicates the ideal state of human beings in harmony with the whole world. The character, Da, reflects open mind with the extended strokes.

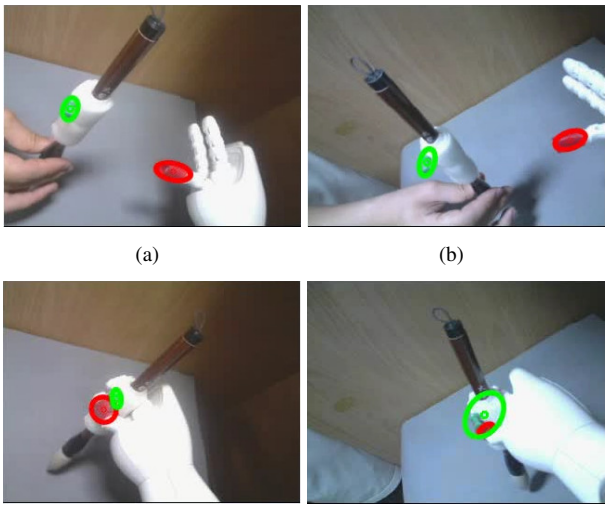

(a) (b)

(c) (d)

Fig. 8 Images captured by two cameras before and after grasping. (a) is from left camera before grasping; (b) is from right camera before grasping; (c) is from left camera after grasping; (d) is from right camera after grasping.

Fig. 9 Chinese characters written by the NAO robot.

3 Conclusion and future work

This paper proposes a visual servoing system for performing Chinese calligraphy with a humanoid robot. The visual servoing controller in this system is based on Kalman-Bucy filter and is robust to the inaccuracy of the system modeling with the help of the object detector by CAMShift algorithm. With the proposed approach, the NAO robot performs satisfactorily in the experiment of writing Chinese characters. Moreover, the results of the experiment indicate the robustness of the algorithm to the noises in images, disturbances on motion system and irregular object motion.

In the future, we hope to enhance the robot's ability of recognizing the object and grasping it from an appropriate attitude. In addition, the humanoid robot is expected to learn how to write different strokes without demonstration but with help from humans through interaction. Further work will also be done on improving the robot's intelligence to recognize every stroke in a Chinese character. The humanoid robot will perform Chinese character like human beings if these ideas come true.

Acknowledgements

Special thanks to Meng Zhang and Lu Wang for countless discussions and feedback leading to the development of this work. Many thanks to Yue Zhao and Rui Chen for their advise on our research topic and their help in implementing the experiments.

References

[1] Robins B, Dautenhahn K, Dickerson P. From isolation to communication: a case study evaluation of robot assisted play for children with autism with a minimally expressive humanoid robot. *Proceeding of the 2009 IEEE International Conferences on Advances in Computer-Human Interactions*, Cancun, 2009, 205 – 211.

[2] Xia G, Dannenberg R, Tay J, Veloso M. Autonomous robot dancing driven by beats and emotions of music. *Proceedings of the 2012 International Conference on Autonomous Agents and Multiagent Systems*, Valencia, 2012, 1: 205 – 212.

[3] Barakova E I, Vanderelst D. From spreading of behavior to dyadic interaction-a robot learns what to imitate. *International Journal of Intelligent Systems*, 2011, 26(3): 228 – 245.

[4] Wainer J, Dautenhahn K, Robins B, et al. Collaborating with kaspar: Using an autonomous humanoid robot to foster cooperative dyadic play among children with autism. *Proceedings of the 2010 IEEE International Conference on Humanoid Robots*, Nashville, 2010, 631 – 638, .

[5] Lo K W, Kwok K W, Wong S M, et al. Brush footprint acquisition and preliminary analysis for Chinese calligraphy using a robot drawing platform. *Proceeding of the 2006 IEEE International Conference on Intelligent Robots and Systems*, Beijing, 2006, 5183 – 5188.

[6] Yao F, Shao G. Modeling of ancient-style chinese character and its application to ccc robot. *Proceedings of the 2006 IEEE Intenational Conference on Networking, Sensing and Control*, Lauderdale, 2006, 72 – 77.

[7] Yao F, Shao G, Yi J. Extracting the trajectory of writing brush in Chinese character calligraphy. *Engineering Applications of Artificial Intelligence*, 2004, 17(6): 631 – 644.

[8] Lam J H M, Yam Y. Stroke trajectory generation experiment for a robotic Chinese calligrapher using a geometric brush footprint model. *Proceedings of the 2009 IEEE Intenational Conference on Intelligent Robots and Systems*, St. Louis, 2009, 2315 – 2320.

[9] Zhang K, Su J. On Sensor Management of Calligraphic Robot. *Proceedings of the 2005 IEEE Intenational Conference on Robotics and Automation*, Barcelona, 2005, 3570 – 3575.

[10] Vahrenkamp N, Asfour T, Dillmann R. Simultaneous grasp and motion planning: humanoid robot ARMAR-III. *IEEE Robotics and Automation Magazine*, 2012, 19(2): 43 – 57.

[11] Tsuji T, Kaneko K, Harada K, et al. Humanoid robot that achieves bipedal walk, visual recognition, and multiple finger grasp. *Proceedings of the 2011 IEEE Intenational Conference on Humanoid Robots*, Bled, 2011, 75 – 80.

[12] Dogar M R, Hsaio K, Ciocarlie M, et al. Physics-based grasp planning through clutter. *Proceedings of Robotics: Science and Systems*, Sydney, 2012.

[13] Kroemer O B, Detry R, Piater J, et al. Combining active learning and reactive control for robot grasping. *Robotics and Autonomous Systems*, 2010, 58(9): 1105 – 1116.

[14] Hutchinson S, Hager G D, Corke P I. A tutorial on visual servo control. *IEEE Transactions on Robotics and Automation*, 1996, 12(5): 651 – 670.

[15] Piepmeier J A, Lipkin H. Uncalibrated eye-in-hand visual servoing. *The International Journal of Robotics Research*, 2003, 22(10-11): 805-819.

[16] Qian J, Su J. Online estimation of image jacobian matrix by kalman-bucy filter for uncalibrated stereo vision feedback. *Proceedings of the 2002 IEEE Intenational Conference on Robotics and Automation*, Washington, 2002, 1:562 – 567.

[17] Bradski G R. Computer vision face tracking for use in a perceptual user interface. *Preceeding of the 1998 IEEE Workshop Application of Computer Vision*, 1998, 214 – 219.

[18] Gouaillier D, Hugel V, Blazevic P, et al. Mechatronic design of NAO humanoid. *Proceedings of the 2002 IEEE Intenational Conference on Robotics and Automation*, Washington, 2002, 769 – 774.

[19] Cheng Y. Mean shift, mode seeking, and clustering. *IEEE Transactions on Pattern Analysis and Machine Intelligence*, 1995, 17(6): 790 – 799.

Ma Zhe was born in 1988. She received her B.S. degree from Xi' An Jiao Tong University in 2010. Her research interests include visual servoing control and human robot interaction.